Edelweiss Applied Science and Technology
ISSN: 2576-8484
Vol. 9, No. 3, 2828-2842
2025
Publisher: Learning Gate
DOI: 10.55214/25768484.v9i3.5880

Numerical investigation changing airflow direction and incoming particle size to reduce residence time in spray dryer

Henry Carles[1,2*], Eflita Yohana[1], Mohamad Djaeni[3], Mohammad Tauviqirrahman[1], Shofwan Bahar[1], Eka Dharmawan[1], Kwang- Hwan Choi[4]
[1]Mechanical Engineering Department, Diponegoro University, Jl. Prof. Soedarto, SH., Semarang 50275, Indonesia; carlesup98@gmail.com (H.C.).
[2]Department of Mechanical Engineering, Faculty of Engineering, Mercu Buana University, Jl. Meruya Selatan no.1, Jakarta Barat 11650, Indonesia.
[3]Chemical Engineering Department, Diponegoro University Jl. Prof. Soedarto, SH., Semarang 50275, Indonesia.
[4]College of Engineering, Pukyong National University 365 Sinseon-ro, Nam-gu, Busan 608-739, Republic of Korea.

Abstract: Spray drying is appropriate for the desiccation of pharmaceutical and alimentary items. Numerical studies with computational fluid dynamics (CFD) on spray dryers can estimate results comparable to experimental methods, so they are widely used in spray dryer research. This numerical simulation aims to examine the correlation between alterations in the input direction from co-current to mixed flow, with differences in temperature and droplet size, and their impact on the residence duration of particles inside the drying chamber, using the k- ω SST turbulence model to simulate the flow, and the standard k- ε to predict particles. In mixed flow, small-diameter droplets (10 and 30 μ m) have a longer particle residence time (9.4 and 4.4 seconds) than in co-current flow; on the other hand, it becomes faster ($\leq$1.2 seconds) for droplet diameters $\geq$50 μ m. Spraying droplets in a mixed flow spray dryer will reduce the residence time of particles relative to co-current flow; larger droplet diameters result in shorter residence times.

Keywords: *Co-current flow, Droplet size, Mixed flow, Residence time, Spray dryer.*

1. Introduction

Spray drying is a technological method that transforms liquids into dry particles using heated drying medium. Anandharamakrishnan, et al. [1] and Wang and Selomulya [2] commonly used in food and pharmaceutical processing [3, 4]. In the drying process, the number of particles coming out of the channel is less than that attached to the wall Mujumdar [5] more small diameters come out of large diameters Dewi and Satibi [6] and Habtegebriel, et al. [7] with the same droplet particle size being removed for each configuration. Countercurrent flow is particle flow opposite to airflow, co-current flow is unidirectional, and mixed flow combines the two [8, 9]. This numerical simulation study aims to assess the impact of variations in inlet droplet diameter on particle residence time, considering temperature fluctuations and the transition of airflow direction from a co-current model to a mixed flow model, as well as to compare particle residence time in the spray dryer for both intake airflow models. In Anandharamakrishnan, et al. [1] research, the results obtained are relatively similar, comparing the experimental results and calculations [1, 3]. The CFD study of the spray dryer forecasts results that are comparably favorable to the experimental method. Elevating the drying air temperature helps reduce the drying duration since the moisture content diminishes rapidly; As a result, the distance to the atomization source will be shorter Habtegebriel, et al. [7] so that the size of the spray dryer will be smaller.

History: Received: 17 January 2025; Revised: 10 March 2025; Accepted: 14 March 2025; Published: 29 March 2025
* Correspondence: carlesup98@gmail.com

Fluid flow characteristics are parameters that determine the performance of the spray dryer. The turbulence models often used in spray dryers include the k-ε model, the k-ω model, and the Reynolds Stress Model (RSM). According to Jubaer, et al. [10] and Weber, et al. [11] the use of turbulence models in the spray-dryer impacts the precision of the airflow attributes inside the drying chamber [8,10]. This study used a spray dryer modified with a drying air inlet to obtain a mixed flow. Its position, located on the upper edge of the drying chamber, causes the incoming air to form a rotating flow like a tangential vortex. From several references, rotating flow modelling usually uses the Reynolds Stress Model (RSM) and Large-Eddy Simulation (LES) methods mainly due to the fact that they are more accurate than the Eddy Viscosity Models (EVMs) approach, but they need more complicated computer specs [11-13]. Another turbulence model is k-ω SST, which is more accurate in rotating flow modeling when compared to the k-ε turbulence model [10, 14]. For the co-current spry dryer, Due to the fact that the fluid flow characteristics on the spray-dryer wall are more realistic when compared to the k-ε RNG turbulence model that has been developed, the standard k-ε turbulence model is used [1, 7, 15, 16].

In Mujumdar's study, in the process of spray drying, there were three different kinds of air and droplet interaction systems which were utilized: co-current, counter-current, and mixed [5]. To atomize particles in the direction of airflow, a co-current spray drier is used. The process of particle atomization in countercurrent spray dryers is the opposite of the airflow than in conventional spray dryers. Co-current and countercurrent flow are both used in the operation of mixed flow spray dryers. This research is to examine the differences and similarities between the mixed flow and co-current particle contact systems.

During the drying process, the features of the spray dryer's exit will be influenced by the temperature of the input as well as the amount of time particles spend in the drier. Increasing the drying air temperature will reduce the resulting product's water content and water activity [16, 17]. In accordance with the findings of Alfonso, et al. [18] and Roustapour, et al. [19] experimental research is To generate a product with a lower moisture content, faster drying time, and shorter distance to the atomization center, raising the temperature of the drying air will result in a rise in the output temperature [19, 20].

The results of the research of Benavides-Morán, et al. [21] When compared to the proportion of particles that are expelled from the spray dryer duct, the percentage of particles that are encountered by the walls of the drying chamber is much higher [21]. The percentage of small-diameter particles that come out of the spray dryer is greater than that of large-diameter particles; This is because small diameter particles have a little momentum, so they are not able to get out of the center of the airflow and tend to follow the direction of the airflow towards the outlet [19, 22].

Modifying the inlet dry airflow direction from unidirectional flow to the mixed flow model can reduce particle residence time. Overall numerical simulation results with 3-dimensional modeling for mixed flow using CFD (Computational Fluid Dynamics) are expected to obtain a reduction in particle residence time to control the quality of dry particle products produced in spry drying processes.

2. Methodology

2.1. Governing Equation

One of the most important factors that determines the outcome of the drying process is the temperature of the hot air that is taken in. Habtegebriel, et al. [7]. Research Arepally and Goswami [16] studied the impact of the spray drying technique's intake drying temperature on the drying process. The spray-drying process was modeled using the computational fluid dynamics (CFD) approach in Ansys Fluent. Findings demonstrate that drying air temperature has an effect on product water content reduction and water absorption.

The interactions between phases in a spray drying system may be explained using one of two multiphase modeling approaches: the Eulerian-Eulerian method or the Euler-Lagrangian approach. A

Edelweiss Applied Science and Technology
ISSN: 2576-8484
Vol. 9, No. 3: 2828-2842, 2025
DOI: 10.55214/25768484.v9i3.5880

three-phase solution flow is the focus of this study, which employs the Eulerian-Lagrangian method to forecast and trace spray-dried particle locations. In the Eulerian-Lagrangian model, the air is continuous and discrete Habtegebriel, et al. [7] on the particles acting gravitational force and drag. In the gas phase, the Lagrangian analysis is used to model particle motion, while the Euler technique is used to solve the Navier-Stokes equation.

These three equations describe the energy, momentum, and continuity of incompressible fluid flow[23]:

$$\rho + \rho(\nabla . \vec{v}) = 0 \tag{1}$$

$$\rho \frac{D\vec{V}}{Dt} = -\nabla p + \rho \vec{g} + \mu(\nabla^2 \vec{V}) \tag{2}$$

$$\rho . c_{pf} . v . \nabla T = \nabla(\lambda_f . \nabla T) + \mu\phi \tag{3}$$

We utilized the discrete phase model (DPM) to count and monitor each particle in the flow path. The particles in the spray-dryer model are assumed to be spherical and non-rotating, with no interparticle interactions and no influence on the fluid flow field (one-way coupling). This leads to the formulation of the particle motion equations in equations 4 and 5 [24].

$$\frac{dx_p}{dt} = \vec{u}_p \tag{4}$$

$$\frac{d\vec{u}_p}{dt} = F_d(\vec{u} - \vec{u}_p) + \vec{g}_x \frac{(\rho_p - \rho)}{\rho_p} \tag{5}$$

Fluid velocity $(\vec{u})$, particle velocity $(\vec{u}_p)$, x_p denotes the location of the particle, $\vec{g}_x$ is the gravitational force, ρ fluid density, and ρ_p shows the density of particles. In Equation (5), $F_d(\vec{u} - \vec{u}_p)$ particle drag per unit mass. F_d is calculated based on Equation 3:

$$F_d = \frac{1}{\tau_p} \frac{(C_d - Re_p \quad)}{24} \tag{6}$$

where (τ_p) the relaxation time of the particle, is given by Equation 7

$$\tau_p = \frac{\rho_p d_p^2}{18\mu} \tag{7}$$

The drag coefficient(C_d) in equation 6 is a function of the particle's Reynolds number, determined by Equation 8 [22].

$$Re_p = \rho d_p \frac{|\vec{u} - \vec{u}_p|}{\mu} \tag{8}$$

In order to get the drag coefficient for spherical particles by using the Morsi and Alexander correlation equation Morsi and Alexander [25] using the relative Reynolds number of particles (Re_p) as provided by Equation 9 and the values a_1, a_2, and a_3 that result from it.

$$C_d = a_1 + \frac{a_2}{Re_p} + \frac{a_3}{Re_p} \tag{9}$$

Edelweiss Applied Science and Technology
ISSN: 2576-8484
Vol. 9, No. 3: 2828-2842, 2025
DOI: 10.55214/25768484.v9i3.5880

Predicting the temperature and moisture content of the dry product particles is made possible in DPM by using the species transport model, which predicts the heat transfer and mass transfer between the particles and the drying air throughout the drying process. Using equation 10, we can express the heat transfer equation as:

$$\frac{d}{dt}\left(m_p c_p T_p\right) = hA_p\left(T_g - T_p\right) + \frac{dm_p}{dt} h_{fg} \tag{10}$$

where m_p mass of particle, c_p is specific heat of the particles, T_p is temperature of particles, The heat transfer coefficient is denoted by h, the particle's surface area is A_p, and the big latent heat of vaporization is h_{fg}.

A mass transfer rate equation is required to forecast the rate of particle evaporation as the temperature of the particles approaches the boiling point and evaporation temperature. Using Equation 11, we can calculate the evaporation rate, which is the rate at which mass transfers from gas to particles:

$$\frac{dm_p}{dt} = -k_c A_p\left(Y_s^* - Y_g\right) \tag{11}$$

In order to determine the vapor concentration on the particle surfaces in the rapid dryer, it is assumed that the partial vapour pressure is equal to the saturated vapour pressure at a given temperature. Equation 12 gives the vapour concentration of the air as it dries.

$$Y_g = X_i \frac{P_{op}}{RT_\infty} \tag{12}$$

P_{op}represents the operational pressure of the drying process. Equation 13 yields the Sherwood number, which is used to calculate the mass transfer coefficient (k_c) in Equation 11:

$$Sh = \frac{k_c d_d}{D_{i,m}} = 2.0 + 0.6\, Re^{\frac{1}{2}} S\, c^{\frac{1}{3}} \tag{13}$$

The variables in Equation 8 are the Sherwood number symbol (Sh), the Schmidt number (Sc), the particle diameter (d_d), the diffusion coefficient (, $D_{i,m}$), and the Reynolds number (Re).

When the spray-dried particles reach their boiling point, we can use Equation 14 to get the model's boiling rate.

$$\frac{dd_p}{dt} = \frac{4k_{ta}}{\rho_p c_g d_p}\left(1 + 0.23\sqrt{Re}() \, ln\left[1 + \frac{c_g\left(T_g - T_p\right)}{h_{fg}}\right]\right) \tag{14}$$

The gas's specific heat capacity (Sc) and thermal conductivity (k_{ta}) are two important parameters to consider.

2.2. CFD Model and Geometry

A spray dryer is good if the design can maximize the use of heat and the particles are dry before hitting the wall [5]. During drying, droplets come into contact with the air currents in three different ways: co-current, countercurrent, and mixed flows. The direction of the incoming airflow affects the speed distribution in the drying process so that it has an impact on the quality of the final product. This study simulates two different spray dryer air input models with identical geometries. Both models depict the airflow into the spray dryer; one shows mixed flow from the top, while the other shows parallel flow from the droplets.

This simulation uses ANSYS Fluid Flow (FLUENT) software to solve numerical equations. The method used is SIMPLE for pressure-speed coupling because it reaches convergence faster. We can forecast the distribution of velocities and temperatures using the second-order approach for discretizing

Edelweiss Applied Science and Technology
ISSN: 2576-8484
Vol. 9, No. 3: 2828-2842, 2025
DOI: 10.55214/25768484.v9i3.5880

pressures. Separation of first-order schemes for kinetic energy, dissipation rate, and momentum. In order to differentiate the Energy equations and prevent numerical instability while improving convergence, a first-order upwind approach is used. For each solution variable, the $1x10^{-4}$ convergence criteria are found; for the energy equation, it is $1x10^{-6}$.

2.2.1. Spray Dryer Geometry

The spray dryers with mixed flow (Figure 1.a) and co-current flow (Figure 1.b) were designed using SolidWorks, and size of the detailed geometry are shown in Table 1.

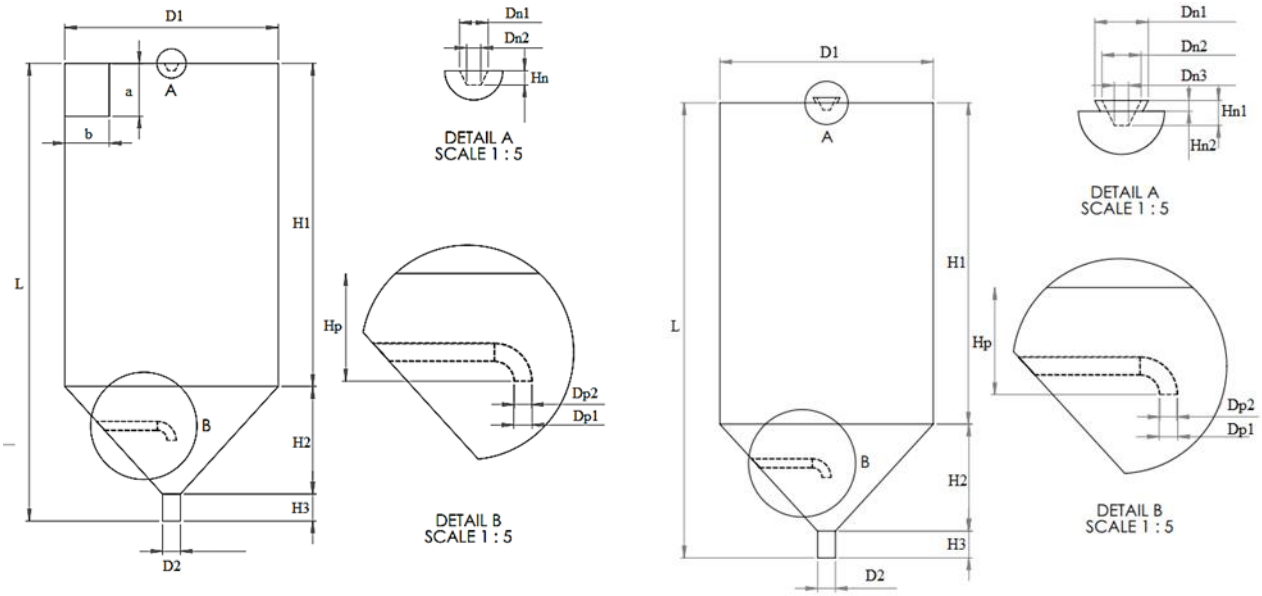

(a) **(b)**

Figure 1.
The dimensions of spray dryer with (a) Mixed flow, (b) Co-current flow.

Table 1.
The dimensions of spray dryer with mixed flow.

No	Geometry	Dimensions (mm)	
		Mixed Flow	Co-current Flow
1	Body radius, D1	300	300
2	Cylinder radius, D2	25	25
3	Nozzle radius 1, Dn1	20	40.5
4	Nozzle radius 2, Dn2	10	27.5
5	Nozzle radius 3, Dn3	-	10
6	Pipe radius 1, Dp1	13	13
7	Pipe radius 2, Dp2	12	12
8	Inlet dimension, a×b	147×125	-
9	Height of the cylinder, H1	900	900
10	Height of the cone, H2	300	300
11	Height of the cylinder, H3	480	480
12	Height of nozzle, Hn	20	-
13	Height of nozzle 1, Hn1	-	35
14	Height of nozzle 2, Hn2	-	15
15	The distance from the pipe to the cylinder, Hp	150	150
16	Spray dryer height, L	1275	1275

2.2.2. Boundary Conditions

Inlet speed, wall, which refers to the surface of the spray dryer and the output pipe, and pressure outlets are the boundary conditions that are established. Drying air inlet speed 8 m/s, hydraulic diameter 0.1351 m, turbulence intensity 3.94, intake air temperature (100°C, 120°C, 140°C, 160°C, dan 180°C), mass loading value 0.0015 kg/s, particle density 816.4 kg/m^3, the density of the gas is 1,225 kg/m^3. Setting the boundary conditions of the spray dryer surface wall as DPM escape and reflecting pipe wall.

To see the distribution and particle size, Rosin-Rammler and PDS (Particle Size Distribution) are used, which assumes the particle diameter and particle fraction exponential relationship shown in equation 15 below[26]:

$$Y_d = e^{\left(\frac{d}{\bar{d}}\right)^n} \tag{15}$$

d represents the particle size, which is measured in millimeters, $\bar{d}$ represents the average diameter of the particles, also measured in millimeters, and n represents the dispersion diameter, which is determined by equation 16, [26]:

$$n = \frac{ln(-ln\, y_d)}{ln(d/\bar{d})} \tag{16}$$

Regarding this particular issue, the particle size ranges from 10 μm to 130 μm, and the diameter of the particles is 50 μm.

2.3. Mesh and Grid Independent Analysis

As can be seen in Figure 2, the size of the elements is used to alter the form and size of the geometry when meshing the spray-dryer geometry using ANSYS Mesh. This is accomplished by utilizing a numerical grid of tetrahedral cells.

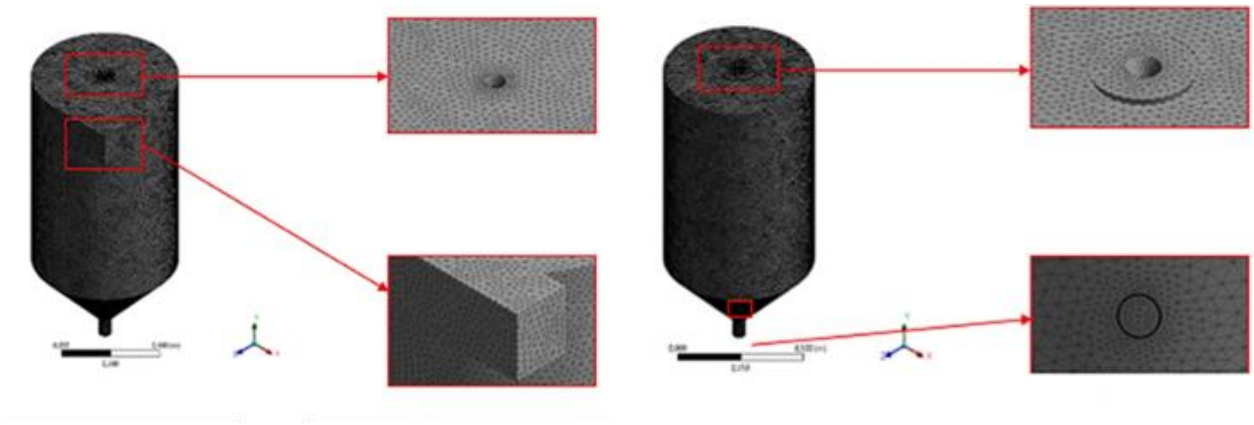

(a) **(b)**

Figure 2.
The structure of the meshing (a) Mixed flow spray dryer (b) Co-current flow spray dryer.

The geometric meshing structure determines the quality of the numeric grid cells, and the indicators are the skewness value and the orthogonal quality. In this study, the output temperature of the spray dryer was calculated with a grid size variation of 0.015 m to 0.013 m at the same limits and operating conditions as the reference used. If appropriate, it will be continued at the stage of the solver

process; for better results, be sure to use a smaller grid size and grid independence in calculations and analysis.

Grid values of 0.0130, 0.0135, 0.0140, 0.0145, and 0.0150 provide Output Temperature (°C) readings of 32.39, 33.09, 32.89, 32.73, and 34.56, respectively. From the simulation results, if the grid size is below 0.0145 m (medium mesh category), the output temperature of the spry dryer does not change (less than 5%). From this, it can be concluded that the independent grid is 0.0145 m in size to be used as a reference for simulation.

2.4. Verification of the Numerical Model

Verification is necessary to ascertain the precision of the used approach. Verification is achieved by juxtaposing the outcomes of numerical simulations with experimental data, using references under identical circumstances. Figure 3 illustrates the corroboration of numerical simulation outcomes with experimental findings from the study conducted by Habtegebriel, et al. [7] as seen in Figure 3a for the output temperature and Figure 3b for the moisture content. Even with a variance of 9.23%, the simulation results show that the reference output of temperature and water content is still within acceptable ranges (maximum 10%). Finally, this technique will be used in simulations to forecast the temperature and residence duration of the particles' output.

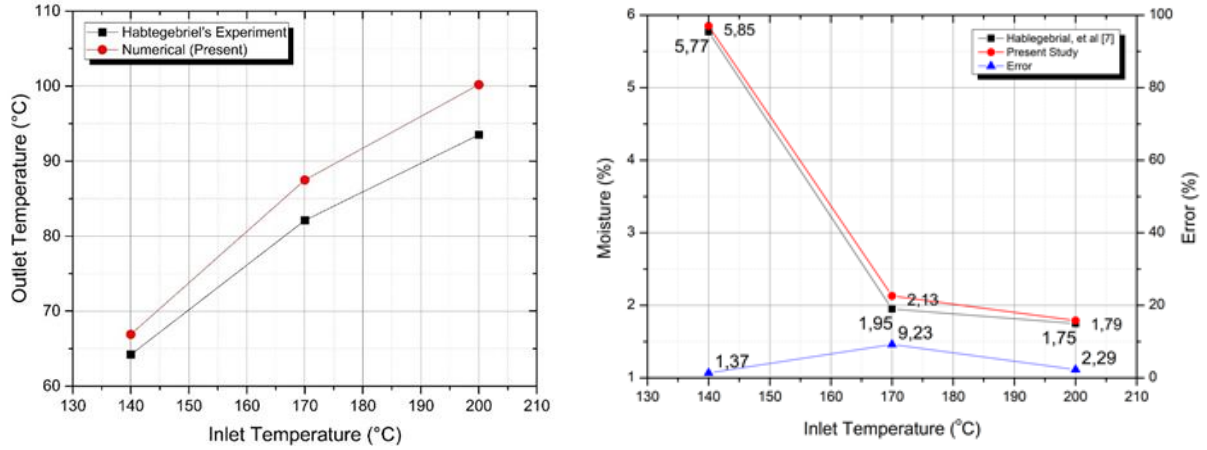

Figure 3.
Validation of numerical and experimental results for (a) outlet temperature and (b) moisture content.
Source: Habtegebriel, et al. [7]

3. Results

3.1. Effect of Drying Air Velocity on Velocity Distribution Characteristics of Spray Dryer

Inside the drying chamber, identification of the airflow velocity distribution, the behaviour of the drying air movement, and the parameters that affect the behaviour of the particle residence time are carried out. Figure 4 compares the velocity contours of mixed flow (Fig. 4a) and co-current flow (Fig. 4b) in a spray dryer.

Edelweiss Applied Science and Technology
ISSN: 2576-8484
Vol. 9, No. 3: 2828-2842, 2025
DOI: 10.55214/25768484.v9i3.5880

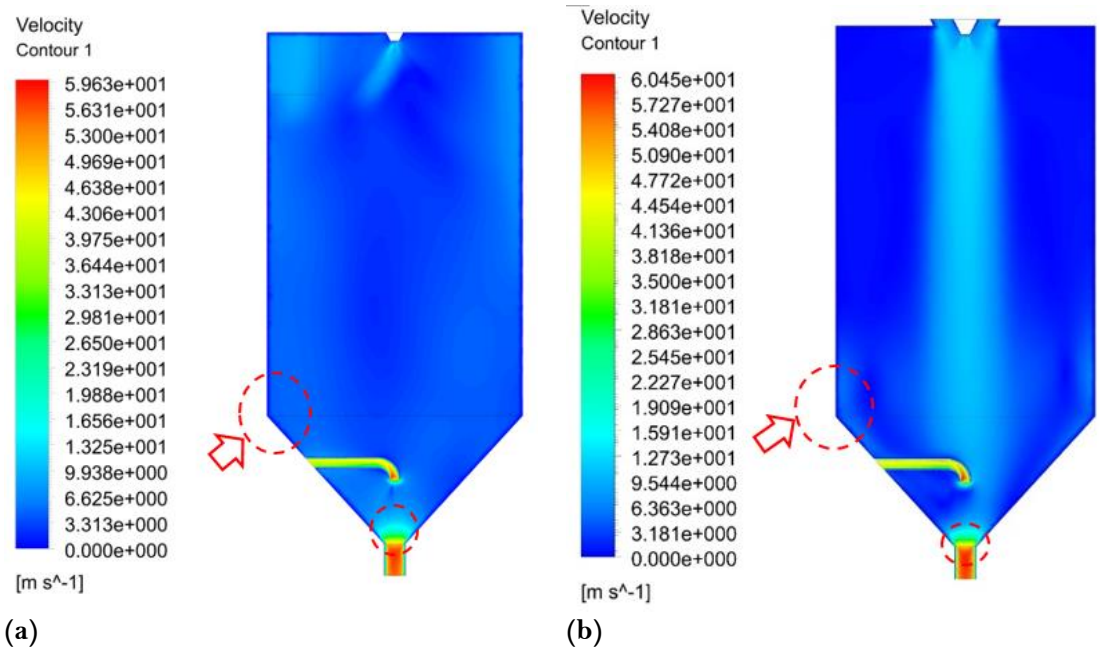

Figure 4.
Spray dryer velocity curve comparison in the drying chamber (a) Mixed flow and (b) Co-current flow.

The air input of the spray drier will influence the distribution and velocity inside the drying chamber. In mixed flow, the channel is positioned in the top section of the drying chamber, as seen in Figure 4(a); thus, the airflow velocity at the center is reduced compared to that at the walls. Figure 4(b) illustrates a co-current flow spray dryer, with the intake positioned at the center-top of the drying chamber, aligned parallel to the atomizing nozzle. The distribution and air velocity in the center are greater than those along the walls of the drying chamber. At a height of 0.05 m, co-current flow exhibits an increase in velocity at the interface between the cylinder and the cone, attributed to air recirculation inside the drying chamber and the constricting effect of the cone's geometric configuration Sadripour, et al. [22] as shown in the velocity contour in Fig. 5(b).

The geometric shape of the cone on the lower side of the drying chamber can change the speed of the drying airflow [27]. The shift from a cylindrical to a conical form decreases the surface area in the drying chamber, thereby increasing the airflow velocity during the transition. Figure 4 illustrates an increase in velocity at the transition point from cylindrical to conical shape in the two spray drying flow models. As air enters the conical shape, its velocity progressively diminishes with height due to the distance traveled and the friction among particles near the outlet.

Edelweiss Applied Science and Technology
ISSN: 2576-8484
Vol. 9, No. 3: 2828-2842, 2025
DOI: 10.55214/25768484.v9i3.5880

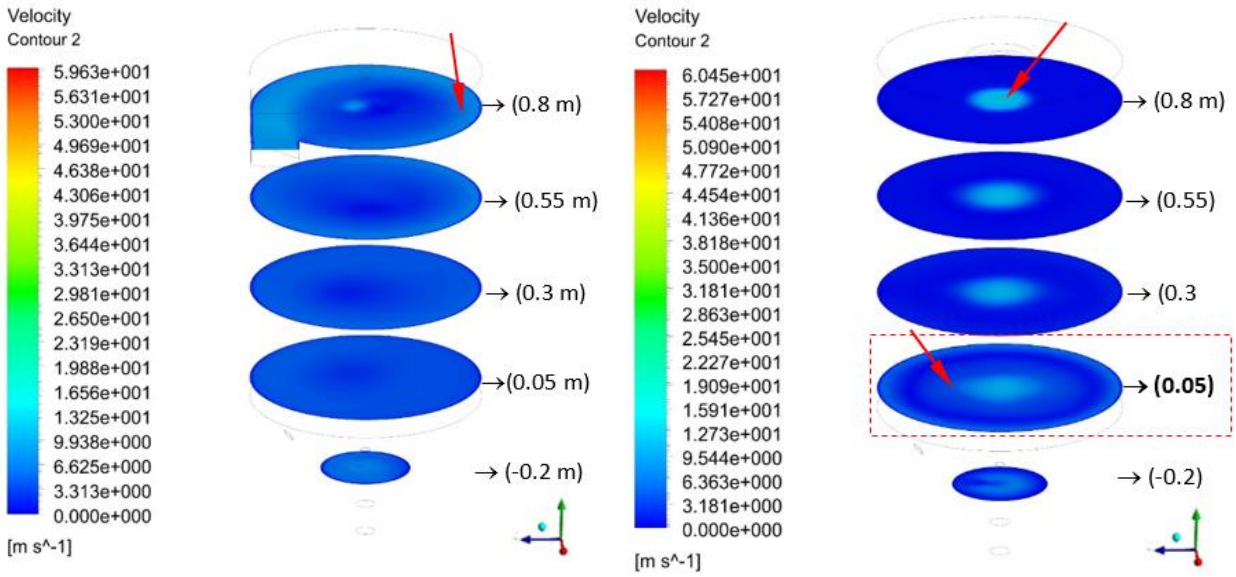

Figure 5.
Within the drying chamber of a spray drier, a comparison of the velocity contours (a) Mixed flow and (b) Co-current flow.

The velocity profiles in the horizontal section of each elevation in the drying chamber for the two varieties of spray dryer flow models are compared in Figures 5 and 6. The airflow velocity of both mixed flow and co-current flow spray dryers decreases as the air travel distance increases at the height of the velocity contour. This condition is by the research conducted by Anandharamakrishnan, et al. [1]; Mezhericher, et al. [15] and Huang, et al. [28].

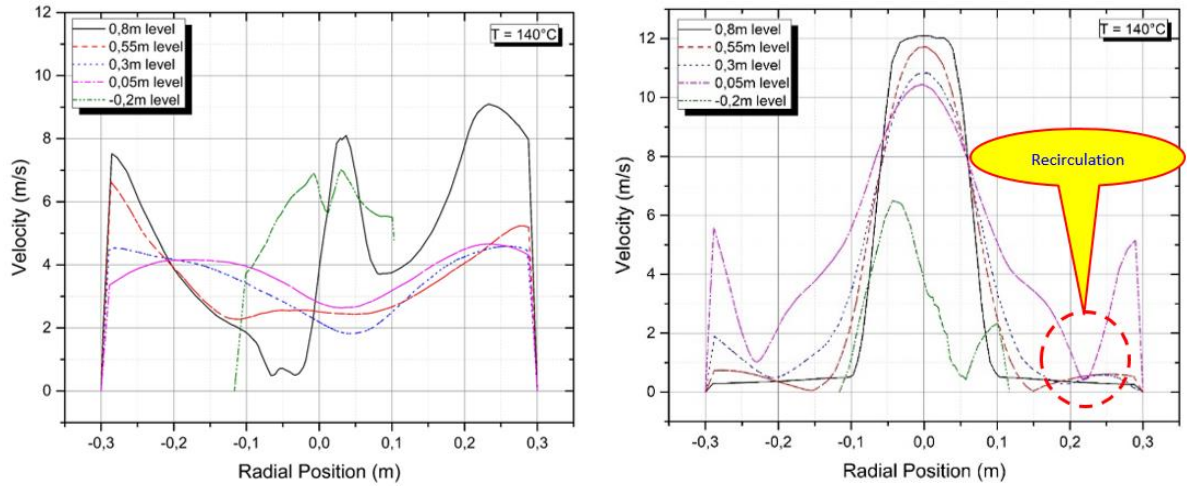

Figure 6.
Velocity graphs compared across all spray drying chamber elevations with (a) mixed flow and (b) co-current flow.

Centrifugally shaped vortexes are formed when air is drawn into the drying chamber of a mixed flow spray drier. At a height of 0.8 m, which is closest to the intake, the drying air velocity is greatest. The air intake of a co-current flow spray dryer is often situated in the center of the upper part of the drying chamber; this allows for a straight path from the inlet to the output, creating a relatively

concentrated area of high air velocity. Particle residence time decreases and outlet temperature rises as a result of direct passage of drying air to the outlet, affecting the quality of the dry product [1, 7]. produced.

The conical form of the drying chamber reduces the lower cross-sectional area, which in turn leads air to recirculate near the walls. As a result, the air velocity near the walls is greater at low altitudes compared to higher elevations. The particles' mobility is improved by the drying chamber's air recirculation, which increases the residence duration of particles for a given diameter. Anandharamakrishnan, et al. [1] found these outcomes in their study [1].

3.2. The X-Center Position's Velocity Distribution and the Streamline Affected by Drying Airflow Velocity

Airflow patterns for mixed flow and co-current in the drying chamber are shown in Figure 7. Because the air intake is located on the side above the spray drier, mixed flow spray dryers have a vortex flow pattern (figure 7. a). The spray dryer's airflow is designed to proceed straight down the drying chamber's output, following the path of the droplet particles. Figure 7b shows how the geometry of the drying chamber transforms from a cylindrical to a conical shape at the connecting point, which then serves as the beginning point for the recirculation of upward airflow that reaches every part of the chamber [1]. The particle characteristics in the drying chamber, such as the distribution of H_2O L mass fraction, relative humidity, and temperature, as well as the quality of the final product, are impacted by the difference in airflow behavior between the two kinds of spray dryers.

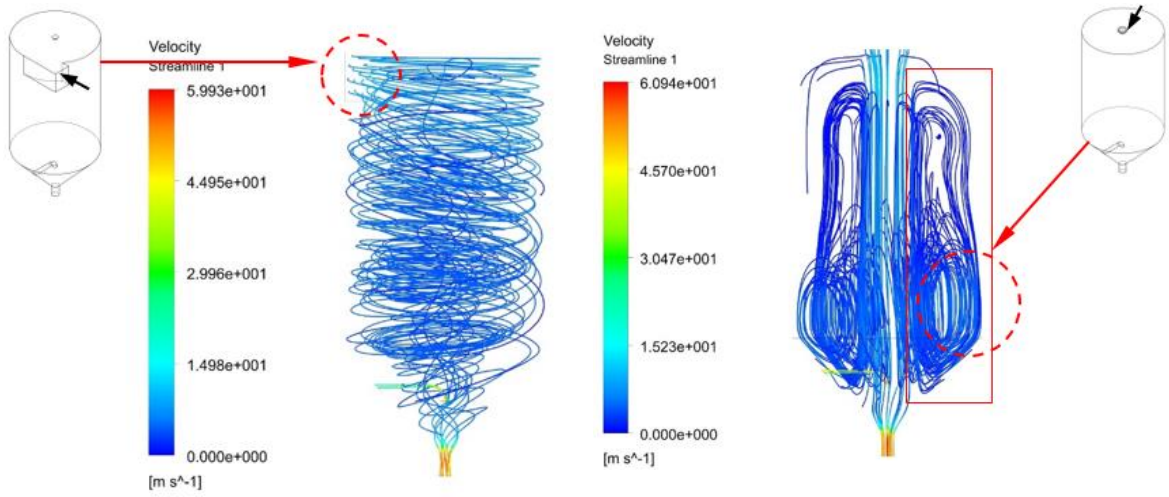

Figure 7.
Velocity stream comparison in the drying chamber (a) Spray dryer with the mixed flow and (b) Spray dryer with the co-current flow.

The flow vectors for the two versions of spray dryers are compared in Figure 8. In Figure 8 (b), the red line region represents the placement of the air recirculation system in a spray dryer that uses co-current flow [15].

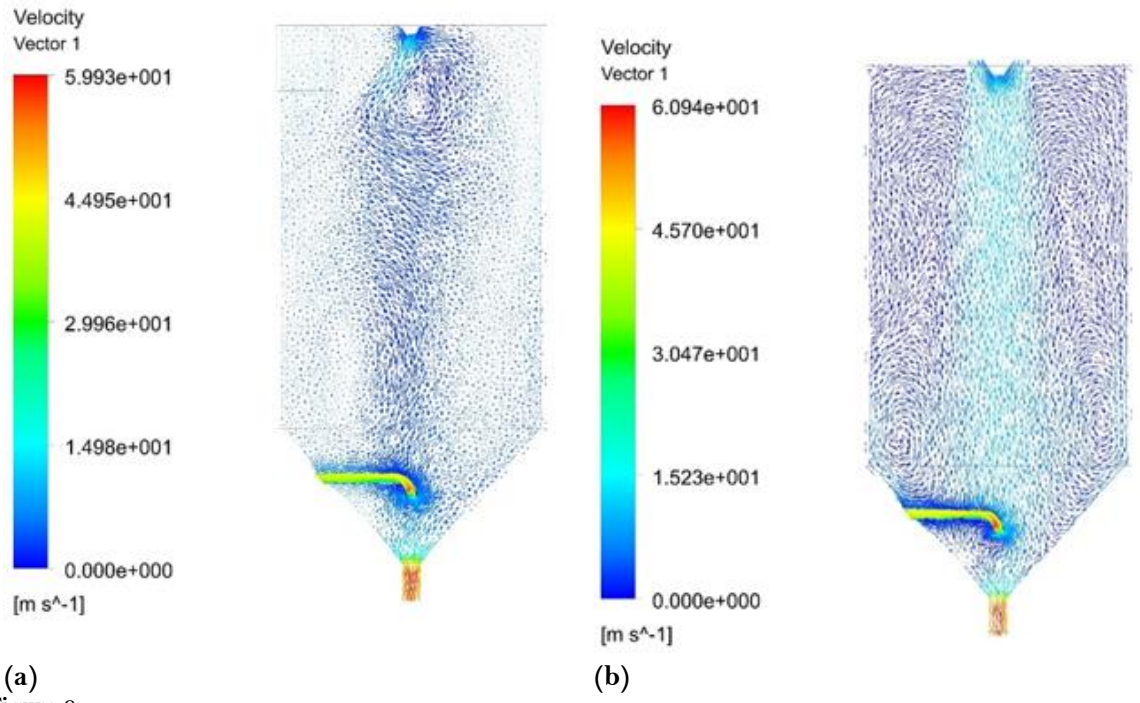

Figure 8.
The drying chamber velocity vector comparison (a) Spray dryer with the mixed flow and (b) Spray dryer with the shared flow.

There are a number of things that happen to the airflow velocity vector in a spray dryer when there is a co-current flow. The large velocity vector is in the middle of the flow centre following the drying airflow pattern entering the outlet, while the smaller air velocity vector tends to be on the right and left sides near the drying chamber wall. Speed is directly proportional to momentum; the greater the velocity, the greater the momentum for constant mass. The drying air velocity vector at the centre of the flow has more significant momentum than outside the centre of the flow on the right and left towards the drying chamber walls, and the momentum tends to be smaller. The velocity vector outside the centre of the flow area forms a vortex pattern, expands and circulates, spreading towards the wall and up, as shown in Figure 8b of vortex-1. The velocity vector progressively diminishes for the flow entering the lower section of the drying chamber. A vortex with a recirculation pattern reemerges at the intersection of cylindrical and conical geometric forms. The Vortex-2 phenomenon arises from a decrease in the surface area resulting from a geometric transformation; hence, the velocity vector will diminish with alterations in altitude. The velocity vector increases again as it exits the outlet on the underside due to the change in geometry from a conical shape to a cylindrical pipe whose diameter is reduced.

3.3. Effect of Airflow Model and Incoming Particle Diameter on Particle Residence Time

The duration that particles remain in the drying chamber throughout the drying process is referred to as particle residence time [1]. In a mixed flow spray dryer, a vortex is created within the drying chamber, generating a centrifugal force. The residence period of the particles diminished from 9.453 s to 0.082 s as the particle diameter increased from 10 µm to 130 µm. For small diameter particles (10 µm and 30 µm), the momentum is very little, making it challenging to leave the vortex; hence, the particles prefer to adhere to the drying airflow pattern, leading to an extended particle residence period. The residence period of particles will be shorter for bigger diameter particles (50 µm, 70 µm, 90 µm, 110 µm, and 130 µm), resulting in comparatively high momentum generation. Particles with substantial momentum can more readily escape the vortex flow, resulting in their collision with the walls of the

Edelweiss Applied Science and Technology
ISSN: 2576-8484
Vol. 9, No. 3: 2828-2842, 2025
DOI: 10.55214/25768484.v9i3.5880

drying chamber [29]. In other words, the particles stay in place faster the faster they go to the exit. These features can be seen in Figure 9, which shows how the link between particle dwell time and particle diameter changes for both mixed and unidirectional flow types.

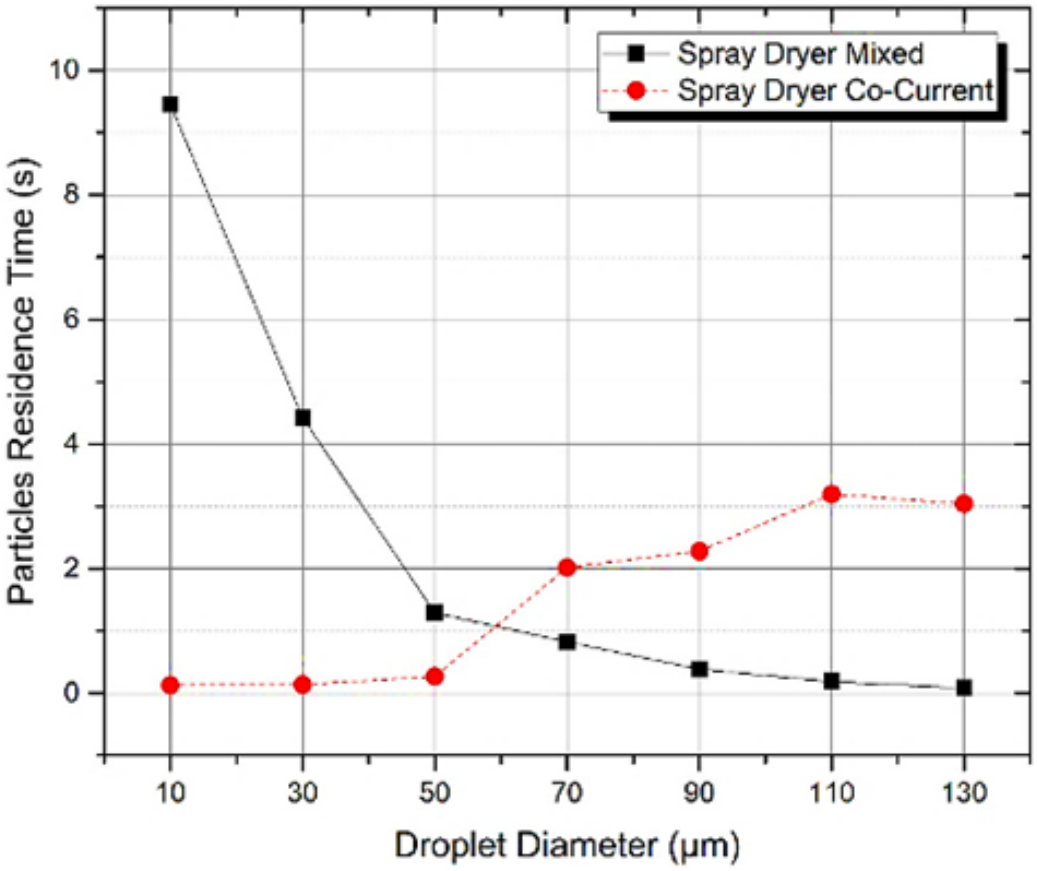

Figure 9.
The length of time that the particles were allowed to remain in the drying chamber.

The atomization process sprays liquid particles, the resulting droplets in the drying chamber have different diameters. The mass of a particle is determined by its diameter, which is directly proportional to the particle's momentum. So that particles with a small diameter have a relatively small momentum. The residence time of particles in a co-current flow spray dryer with large particle diameters (70 μm, 90 μm, 110 μm, dan 130 μm) tends to be longer than those with small diameters (10 μm, 30 μm dan 50 μm); This is because: The small momentum makes the particles unable to leave the flow centre, so the particles tend always to follow the direction of the drying airflow to the outlet and leave the drying chamber faster. On the other hand, for particles with a larger diameter, the momentum is also significant (the mass is large), so the particles are more easily thrown out of the central area of the incoming air stream. The process of ejecting particles from the centre of the flow causes random and irregular movements between particles, resulting in collisions that trigger the growth of circulating vortex patterns. In the area where the cylindrical geometry meets the cone, a vortex with a recirculation pattern occurs again due to the reduction in surface area due to the geometric shape. However, in the radial direction, there is an increase in speed, as well as when exiting the outlet on the bottom side, there is an increase in speed due to a change in geometry from a conical shape to a cylindrical pipe with

Edelweiss Applied Science and Technology
ISSN: 2576-8484
Vol. 9, No. 3: 2828-2842, 2025
DOI: 10.55214/25768484.v9i3.5880

a smaller diameter. Due to collisions between particles, recirculation, the friction of particles with walls, and the gradual descent of particles to lower heights, the velocity of the particles tends to decrease gradually. Under these conditions, the particle velocity is smaller than the airflow velocity, making it more difficult for large diameter particles to penetrate back into the centre of the drying air stream. This condition makes the residence time of large-diameter particles in the co-current flow longer than that of small-diameter particles. The results of this simulation show conformity with the research conducted by Anandharamakrishnan, et al. [1]; Sadripour, et al. [22] and Roustapour, et al. [19] in the end, some large-diameter particles (stuck to the wall) will have the same velocity as the airflow as each velocity changes, with the particle motion pattern and airflow following a conical shape converging downward towards the spray drying outlet.

3.4. Effect of Drying Air Flow Type and Particle Diameter on Distribution of Particle Final Position

The efficiency of particle collection is determined by the percentage of particles that come out of the spray dryer. Research by Anandharamakrishnan, et al. [1] concluded that a spray dryer is efficient if its design and operation method can increase the percentage of particles leaving the outlet. The results of the study of Sadripour, et al. [22] and Roustapour, et al. [19] with a co-current spray dryer, for tiny diameter droplets, the particle momentum is relatively small so that it cannot escape from the centre of the dryer airflow; as a result, the particles tend to rotate in the direction of the drying airflow pattern. The resulting product is dry solid particles; the droplets with small diameters are formed faster than large diameter droplets. Droplets of large diameter particles have a more significant momentum that allows particles to escape from the flow centre, thrown out of the flow centre towards the walls of the drying chamber, which repeatedly occurs due to the flow recirculation phenomenon.

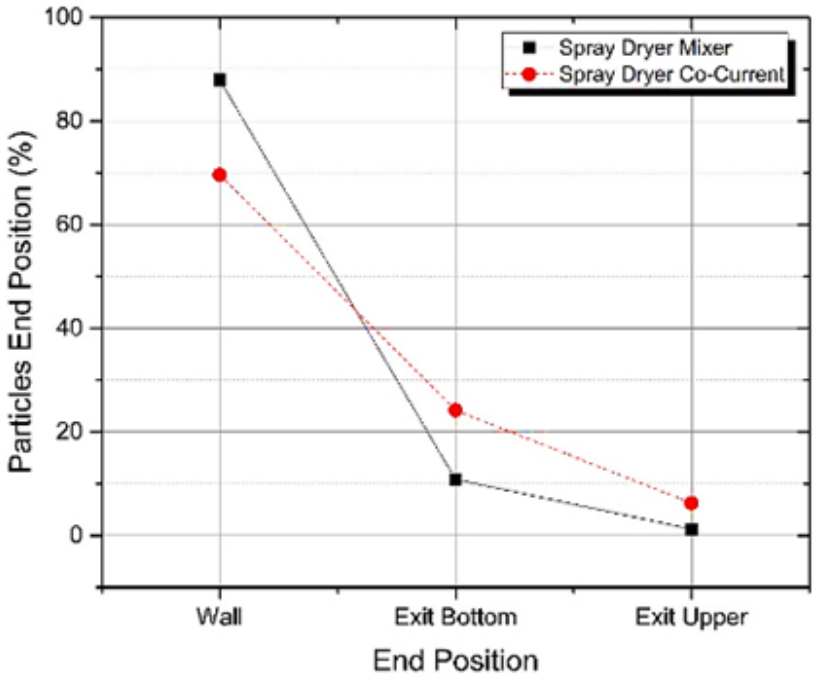

Figure 10.
Total Percentage of Final Position of Particles in Drying Chamber.

Figure 10 shows a graph of the simulation results that compare the percentage of total particles that hit the wall and exit through the channel (top and side positions) for the configuration of the two

Edelweiss Applied Science and Technology
ISSN: 2576-8484
Vol. 9, No. 3: 2828-2842, 2025
DOI: 10.55214/25768484.v9i3.5880

flow models. In the mixed flow spray dryer, dominantly, 87.92% of the particles hit the wall (for co-current flow 69.58%), and the remaining 12.08% exited through the outlet. This is due to the vortex generated in the mixed flow spray dryer so that the tangential velocity is more significant, resulting in a centrifugal force around the drying chamber which causes the particles to hit, rub against and stick to the walls of the drying chamber. On the other hand, in the co-current flow spray dryer, the percentage of total particles coming out of the outlet is 2.5 times more significant efficiency (30.42%) than the mixed flow. The phenomenon of velocity vector recirculation that arises makes some particles forced to follow the pattern so that they collide and rub against the walls of the drying chamber. This causes many particles to stick to the walls because they are not dry enough to become a solid and dry product.

4. Conclusions

This study concludes from the simulation results of multiphase spray dryer modelling, which changes the co-current flow model into a mixture with variations in temperature and droplet diameter that will affect the motion and residence time of the particles. Changes in the diameter of the incoming droplets will change the residence time of the particles during the drying process. Changing the inlet heating airflow from a co-current flow model to a mixed flow model will shorten the residence time of the particles. In mixed flow, the residence time of small diameter droplet particles (10 and 30μm) is longer (9.4 and 4.4 seconds) than in co-current flow; on the other hand, it becomes faster (≤1.2 s) for droplet diameter ≥50μm because the particles follow the vortex pattern of air flow formed by the inlet model. In mixed flow, the larger the inlet droplet, the faster the residence time; On the other hand, for co-current flow, the larger the incoming droplet, the longer the residence time due to the emergence of eddies with particle recirculation patterns in the drying airflow.

Transparency:

The authors confirm that the manuscript is an honest, accurate, and transparent account of the study; that no vital features of the study have been omitted; and that any discrepancies from the study as planned have been explained. This study followed all ethical practices during writing.

Author Contribution:

Henry Carles: Methodology, Study design. Eflita Yohana: Project administration, Writing – review. Mohamad Djaeni: Writing – original draft and editing. Mohammad Tauviqirrahman: Software, Formal analysis. Shofwan Bahar: Validation, Data acuration. Eka Dharmawan: Visualization, Investigation, Resources. Kwang-Hwan Choi: Conceptualization, Supervision.

Acknowledgement:

This research was funded by a grant from the DRPM (Directorate of Research and Community Service) of the Ministry of Research and Technology/BRIN (187-54/UN7.6.1/PP/2021).

References

[1] C. Anandharamakrishnan, J. Gimbun, A. Stapley, and C. D. Rielly, "A study of particle histories during spray drying using computational fluid dynamic simulations," *Drying Technology*, vol. 28, no. 5, pp. 566-576, 2010.

[2] Y. Wang and C. Selomulya, "Spray drying strategy for encapsulation of bioactive peptide powders for food applications," *Advanced Powder Technology*, vol. 31, no. 1, pp. 409-415, 2020.

[3] H. Habtegebriel, D. Edward, M. Wawire, D. Sila, and E. Seifu, "Effect of operating parameters on the surface and physico-chemical properties of spray-dried camel milk powders," *Food and Bioproducts Processing*, vol. 112, pp. 137-149, 2018.

[4] G. Chegini and M. Taheri, "Whey powder: Process technology and physical properties: A review," *Middle-East journal of scientific Research*, vol. 13, no. 10, pp. 1377-1387, 2013.

[5] A. S. Mujumdar, *Handbook of industrial drying*. CRC press, 2006.

[6] A. K. Dewi and L. Satibi, "Kajian pengaruh temperatur pengeringan semprot (spray dryer) terhadap waktu pengeringan dan rendemen bubuk santan kelapa (coconut milk powder)," *Jurnal Konversi*, vol. 4, no. 1, 2015.

[7] H. Habtegebriel, D. Edward, O. Motsamai, M. Wawire, E. Seifu, and S. Daniel, "The potential of computational fluid dynamics simulation to investigate the relation between quality parameters and outlet temperature during spray drying of camel milk," *Drying Technology*, vol. 39, no. 13, pp. 2010-2024, 2021.

[8] H. Jubaer, S. Afshar, J. Xiao, X. D. Chen, C. Selomulya, and M. W. Woo, "On the effect of turbulence models on CFD simulations of a counter-current spray drying process," *Chemical Engineering Research and Design*, vol. 141, pp. 592-607, 2019.

[9] M. Z. Azmi, I. H. Rukunudin, H. A. Ismail, and A. A. Aznan, "Specific energy consumption and drying efficiency analysis of commercial mixed-flow batch type seed drying system," *Journal of Advanced Research in Fluid Mechanics and Thermal Sciences*, vol. 55, no. 1, pp. 39-50, 2019.

[10] H. Jubaer *et al.*, "The impact of self-sustained oscillations on particle residence time in a commercial scale spray dryer," *Powder Technology*, vol. 360, pp. 1177-1191, 2020.

[11] R. Weber, B. Visser, and F. Boysan, "Assessment of turbulence modeling for engineering prediction of swirling vortices in the near burner zone," *International Journal of Heat and Fluid Flow*, vol. 11, no. 3, pp. 225-235, 1990.

[12] O. Hamdy, M. A. Bassily, H. M. El-Batsh, and T. A. Mekhail, "Numerical study of the effect of changing the cyclone cone length on the gas flow field," *Applied mathematical modelling*, vol. 46, pp. 81-97, 2017.

[13] Y. You, F. Seibold, S. Wang, B. Weigand, and U. Gross, "URANS of turbulent flow and heat transfer in divergent swirl tubes using the k-ω SST turbulence model with curvature correction," *International Journal of Heat and Mass Transfer*, vol. 159, p. 120088, 2020.

[14] Y. Liu, Y. Rao, and B. Weigand, "Heat transfer and pressure loss characteristics in a swirl cooling tube with dimples on the tube inner surface," *International journal of heat and mass transfer*, vol. 128, pp. 54-65, 2019.

[15] M. Mezhericher, A. Levy, and I. Borde, "Droplet–droplet interactions in spray drying by using 2D computational fluid dynamics," *Drying Technology*, vol. 26, no. 3, pp. 265-282, 2008.

[16] D. Arepally and T. K. Goswami, "Effect of inlet air temperature and gum Arabic concentration on encapsulation of probiotics by spray drying," *Lwt*, vol. 99, pp. 583-593, 2019.

[17] E. P. Ying, M. Z. Ngali, M. O. M. Z. Azmi, and W. C. An, "Drying droplets: A review on its numerical and experimental studies to remove coffee ring effect," *Journal of Advanced Research in Fluid Mechanics and Thermal Sciences*, vol. 69, no. 1, pp. 46-63, 2020.

[18] F. Alfonso, R. A. Byrne, F. Rivero, and A. Kastrati, "Current treatment of in-stent restenosis," *Journal of the American College of Cardiology*, vol. 63, no. 24, pp. 2659-2673, 2014.

[19] O. R. Roustapour, M. Hosseinalipour, B. Ghobadian, F. Mohaghegh, and N. M. Azad, "A proposed numerical–experimental method for drying kinetics in a spray dryer," *Journal of Food Engineering*, vol. 90, no. 1, pp. 20-26, 2009, doi: https://doi.org/10.1016/j.jfoodeng.2008.05.031.

[20] R. Aguirre-Alonso, M. Morales-Guillermo, M. Salgado-Cervantes, V. Robles-Olvera, M. García-Alvarado, and G. Rodríguez-Jimenes, "Effect of process variables of spray drying employing heat pump and nitrogen on aromatic compound yield in powders obtained from vanilla (Vanilla planifolia Andrews) ethanolic extract," *Drying Technology*, 2019.

[21] A. Benavides-Morán, A. Cubillos, and A. Gómez, "Spray drying experiments and CFD simulation of guava juice formulation," *Drying Technology*, vol. 39, no. 4, pp. 450-465, 2021, doi: https://doi.org/10.1080/07373937.2019.1708382.

[22] M. Sadripour, A. Rahimi, and M. S. Hatamipour, "Experimental study and CFD modeling of wall deposition in a spray dryer," *Drying Technology*, vol. 30, no. 6, pp. 574-582, 2012.

[23] A. M. Noh, S. Mat, and M. H. Ruslan, "CFD simulation of temperature and air flow distribution inside industrial scale solar dryer," *Journal of Advanced Research in Fluid Mechanics and Thermal Sciences*, vol. 45, no. 1, pp. 156-164, 2018.

[24] S. Jayaraju, "Study of the air flow and aerosol transport in the human upper airway using LES and DES methodologies," 2009.

[25] S. Morsi and A. Alexander, "An investigation of particle trajectories in two-phase flow systems," *Journal of Fluid mechanics*, vol. 55, no. 2, pp. 193-208, 1972.

[26] A. Fluent, "Ansys fluent theory guide," in "Ansys Inc., USA," 2011, vol. 15317. [Online]. Available: http://www.afs.enea.it/project/neptunius/docs/fluent/html/th/main_pre.htm

[27] P. J. Pritchard and J. W. Mitchell, *Fox and McDonald's introduction to fluid mechanics*. John Wiley & Sons, 2016.

[28] L. Huang, K. Kumar, and A. Mujumdar, "Simulation of a spray dryer fitted with a rotary disk atomizer using a three-dimensional computional fluid dynamic model," *Drying Technology*, vol. 22, no. 6, pp. 1489-1515, 2004.

[29] L. Brar, R. Sharma, and R. Dwivedi, "Effect of vortex finder diameter on flow field and collection efficiency of cyclone separators," *Particulate Science and Technology*, vol. 33, no. 1, pp. 34-40, 2015.

Edelweiss Applied Science and Technology
ISSN: 2576-8484
Vol. 9, No. 3: 2828-2842, 2025
DOI: 10.55214/25768484.v9i3.5880